sciendo

Civil and Environmental Engineering
Vol. 19, Issue 1, 301-317, DOI: 10.2478/cee-2023-0027

STRUCTURAL BEHAVIOUR OF VOIDED FLAT SLAB WITH VARIOUS VOID RATIOS UNDER VERTICAL LOADING

L. LAKSHMI KANTH[1], P. POLURAJU[2,*]

[1] Research Scholar, Department of Civil Engineering, K L Deemed to be University, Guntur (Dist.), Andhra Pradesh, 522302, India.
[2] Professor, Department of Civil Engineering, K L Deemed to be University, Guntur (Dist.), Andhra Pradesh, 522302, India.
[*] corresponding author: rajupolup@gmail.com

Abstract

In recent modern buildings, voided slabs have been implemented because of the high reduction of their weight up to 35 %. Also, CO_2 emission takes place which was developed from mass concrete. Due to percentage reduction of concrete, it leads to help the pollution free environment, eco-friendly and also more sustainable. On voided flat slabs, a minimal study has been recorded. In this current study, an approach has been made to study the effect of the position of voids in the voided flat slabs. Two groups of seven specimens each, one slab in each group was a controlled flat slab specimen with zero number of voids kept as a reference specimen, while the others were voided slabs. In each group, the number of voids were used based on the positions. The designation of the specimens is made depending on the number of voids placed and the diameter of the rebar used in the specimens. Group-A was reinforced with 8 mm diameter rebars, and Group-B was reinforced with 6 mm diameter rebars. The parameters of the study are the void positions and the rebar diameter. The specimens were subjected to a gradually concentrated load through the short column up to failure. The load carrying capacity of both voided and controlled flat slabs tested have almost same. It indicates that, the inactive concrete below the neutral axis where high density polyethylene (HDPE) recycled hollow spheres have been provided in the flat slab has shown no impact on load carrying capacity of the test specimens. However, the presence of the punching shear can be seen in the specimens where the voids are positioned near the columns and supports. Besides, ABAQUS program (A finite element based software) was used to perform the finite element analysis for profoundly illustrating the experimental findings and performing a parametric study. It is concluded that the concrete has no role at below the neutral axis of structural voided flat slab cross-section for all specimens including controlled specimens (0VS6, 0VS8). Also, it is noticed that the finite element analysis obtained results have shown more or less same as experimental results. From the present study, it is evident that behaviour of voided flat slabs are different from simply supported voided flat slabs.

Keywords:

Voided flat slabs;
High density polyethylene (HDPE);
Eco-friendly;
Mid deflection;
Finite element analysis.

1 Introduction

The dead load of the flat slabs can be reduced by replacing the structurally inactive concrete with High-Density Polyethylene (HDPE) voids. The voided flat slab system incorporates hollow HDPE spheres in the concrete between the bi-axial wire meshes. It contributes to making the voided flat slab sustainable by removing the volume of concrete equal to the replaced voids. The voided flat slabs are light in weight, thin and bidirectional, with a reduction of self-weight up to 35 % [1]. Subsequently, the foundation load on the soil will be minimum, in turn it can reduce the number of columns in a structure.

These are economical with the same slab thickness and substantially reduced volume, which demands lower steel. The voided slabs are earthquake-proof, fire-resistant, and with improved acoustic behavior [2].

Voided slabs were first invented in 1990, a new system of the slab where HDPE spheres are sandwiched between the top and bottom reinforcement and casting is done, which acts as a two-way slab where the load can be transferred in any direction by a Danish Engineer Jorgen, same flexural strength can be obtained with reducing of weight [3] with high load carrying capacity and material saving. Voided slabs are considered sustainable green structures [4].

The voided flat slabs have been classified as three forms, such as Type-A-Filigree elements, Type-B-Reinforcement modules, and Type-C-Finished planks. Out of these three, finished plank type flat slabs are prefabricated and it is quicker construction. As per literature review, voided slabs have many advantages, such as quicker construction period, low cost formwork, optimized structure, and more sustainability to the architectural geometrical requirements like large spans in a structure for the architects instead of conventional reinforced concrete slabs [5]. Consequently, an enhanced seismic performance due to reduced structural mass, therefore, voided slab system, is considered a sustainable solution since the reduction of usage of concrete leads to reduced CO_2 emissions resulting from material production and transportation [6].

Many researchers have investigated various properties such as flexural strength, shear resistance, punching shear, and fire resistance. Chung and associates made research on voided slabs to find the shear capacity with donut-type hollow spheres with test parameters including two different shapes and materials of plastic balls and punching shear design of voided slabs [7]. The shape parameters were donut and non-donut forms, and the material parameters were general plastic and glass fibre plastic [8]. Falah and adnan has studied the punching shear behaviour of fibrous high strength concrete slabs reinforced with Basalt fibre-reinforced polymer (BFRP) bars [9]. Sagadevan [10] made research on punching shear of voided slab. Van along with colleagues assumed the use of elliptical shaped balls and studied the behaviour of voided slabs [11]. Al-gasham and fellows made research on biaxial voided slabs and slab–column connection using steel sheets and quasi static analysis of voided slabs with openings [12].

For the same depth of both the solid slab and voided slab, the flexural strength of the concrete slab is slightly higher than the voided slab, whereas the one-way shear strength of voided slab is 27-40 % below that of the solid slab. The development of the shear cracks depends on the shape of the voids. There is a significant change in the punching shear, with the replacement of voids causing a substantial drop in the punching shear of the voided slab. The punching shear is high when the voids are provided near the support, called the critical section [13]. The emptiness should be eliminated in the critical section to decrease the punching failure. Many more investigations are carried out on voided slabs. Still, from the above literature, it is observed that very few attempts were made on flat slab conditions and several vital issues in the voided slabs have not been discussed to determine the strength of voided slabs depending on the percentage of voids and position of voids. The position of the void also plays a significant role in the structural behaviour of slab. This research mainly focuses on voided flat slabs, with the flat slab boundary conditions which is much less focused by past researchers.

2 Research significance

A few attempts were made on the voided flat slabs to know the effect of the percentage of voids and reinforcement on the behaviour of voided flat slabs. As of now most of the research has been recorded on voided simply supported slabs, whereas in this current study, the voided slabs have been tested with flat slab support conditions. As far as the present study is concerned, only limited investigations were conducted by keeping variables such as the percentage of void ratios and diameter of rebars. However, the studies were not conducted so far on flat slabs by providing flat slab boundary conditions which makes it necessary for an experimental based approach in studying the structural behaviour of concrete voided flat slabs by vertical loading and employing suitable compressive strength of concrete. Therefore, the present research aims to evaluate the behaviour of voided concrete flat slabs with various void positions with a number of voids 0, 12, 16, 20, 24, 32, and 36 under vertical loading. The different configurations of reinforcement details in the voided flat slabs and rebar diameters are 6 mm in Group-A and 8 mm in Group-B were considered as parameters.

3 Experimental program

The present experimental and numerical study have been carried out for voided flat slabs with various void ratios and reinforcement percentages. A total of fourteen flat slabs of size 1000 mm × 1000 m × 150 mm top and bottom reinforcement are provided with rebar diameter 6 mm in Group-A and 8 mm in Group-B are presented in Table 1. The test specimens were cast and tested in the structural engineering laboratory of the Koneru Lakshmaiah Educational Foundation, Vaddeswaram, Guntur (Dist.), Andhra Pradesh, India. The research was targeted to study the effect of void position and the percentage of reinforcement as parameters on the load-carrying capacity of the voided flat slabs. These parameters include two steel rebar diameters and seven different configurations of voids in the voided flat slabs. The specimens are designated as XVSY, where X represents the number of voids and Y represents the diameter of the rebar. Further, VS represents voided slab. The 0VS6 and 0VS8 are the controlled flat slab specimens cast with zero voids. The 36VS8 and 36VS6 are slabs with the maximum number of voids 36, similarly, other slabs also have been designated and presented in Table 1.

Table 1: Details of test specimens.

Group-A	**36VS6**	**32VS6**	**24VS6**	**20VS6**	**16VS6**	**12VS6**	**0VS6**
No. of voids	36	32	24	20	16	12	0
Rebar diameter [mm]	6 mm φ	6 mm φ	6 mm φ	6 mm φ	6 mm φ	6 mm φ	6 mm φ
Average compressive strength cubes [MPa]	28.3	28.3	28.4	28.4	28.1	28.2	28.3
Group-B	**36VS8**	**32VS8**	**24VS8**	**20VS8**	**16VS8**	**12VS8**	**0VS8**
No. of voids	36	32	24	20	16	12	0
Rebar diameter [mm]	8 mm φ	8 mm φ	8 mm φ	8 mm φ	8 mm φ	8 mm φ	8 mm φ
Average compressive strength cubes [MPa]	28.2	28.1	28.0	28.4	28.3	28.2	28.3

3.1 Materials

The M20 grade concrete was taken into consideration for casting the test specimens. The design mix proportions are considered as per IS : 10262-2019 [14] and presented in Table 2. Table 2 demonstrates the constituents required for 1 m^3 of concrete utilization in preparing the concrete mix to get a target mean strength of 26.6 MPa. For every specimen, nine cubes were cast with similar exposure conditions to the slab specimen and tested at the time of slab testing; its strength was presented in Table 1, and the standard deviation was 4 MPa. Table 2 presents the compressive strengths of the concrete cubes 150 mm × 150 mm × 150 mm showing an average of nine standard cubic specimens that were cast and tested under compression at the age of 28 days as a part of the compressive strength test of the concrete cubes, as per IS 456:2000 [15]. The mechanical properties of the TMT Fe500 bars were used as per IS 1608 Part 1: 2018 [16], and values are summarized in Table 3.

Table 2: Mix proportions of concrete trial mix design and test results of cubes.

Mix proportions [kg/m³]					
Design strength [MPa]	**Cement [kg]**	**Coarse aggregate [kg]**	**Fine aggregate [kg]**	**Water [l]**	**Cube compressive strength [MPa]**
26.6	310	697	1394	171	28.8

The reinforcement of 6 mm and 8 mm diameter rebars were having a yield strength of 500 MPa. The sphere void formers are manufactured with recycled polypropylene and are used to form voids in the flat slab specimens. The specifications of the void formers are summarized as a spherical hollow plastic ball of wall thickness 3 mm with 90 mm outer diameter. The voids are used in different numbers and positions with centre-to-centre spacing in longitudinal and transverse directions. The centre-to-centre distance was kept at 166 mm either and the dimensions and details of the actual sphere are shown in Fig. 1. To study the behaviour of voided flat slabs with the position of voids. The reinforcement provided with 6 mm rebar in Group-A and 8 mm rebar in Group-B is used on top and bottom to keep the voids in position with a clear cover of 20 mm at the bottom in individual groups. Fig. 2, shows the actual photograph of voided flab slab in the mould. The configuration of voids in

Group-A and Group-B specimens have shown in Figs. 3a to 3f, the representation of supports at the corners and the short column at the centre also shown.

Table 3: Mechanical properties of reinforcement.

Diameter of reinforcement [mm]	Strength [MPa]			Strain [%]	
	Nominal	Yield	Tensile	Yield	Ultimate
6	500	546	644	0.0032	0.0621
8	500	572	625	0.0036	0.1046

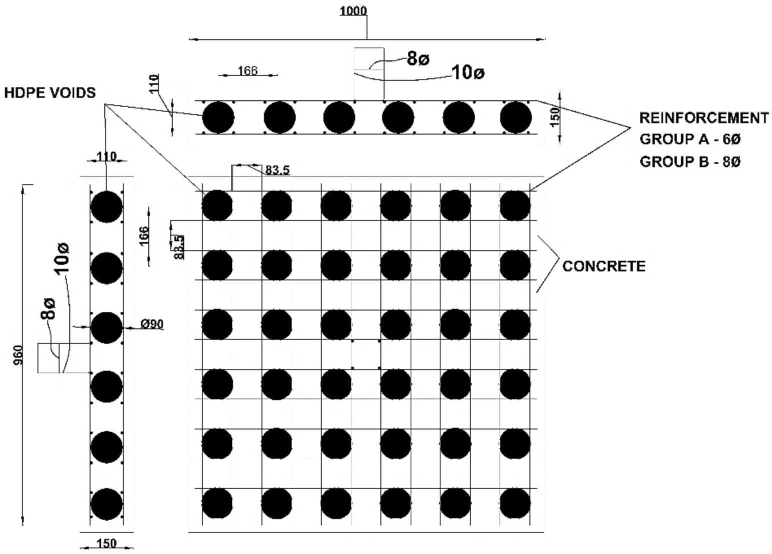

Fig. 1: Details of the arrangement of voids in 36VS8 and 36VS6.

Fig. 2: Actual photograph of voided flat slab in the mould.

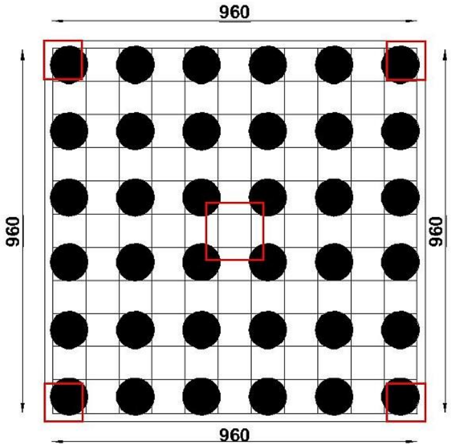

Fig. 3a: Arrangement of voids in 36VS8 and 36VS6.

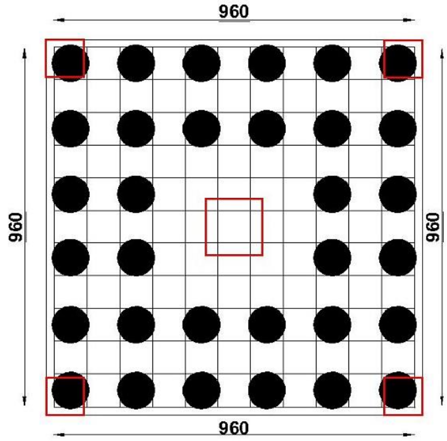

Fig. 3b: Arrangement of voids in 32VS8 and 32VS6.

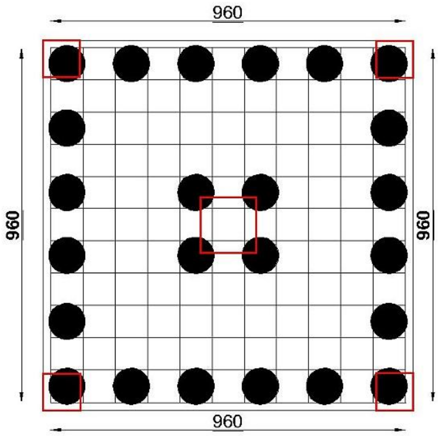

Fig. 3c: Arrangement of voids in 24VS8 and 24VS6.

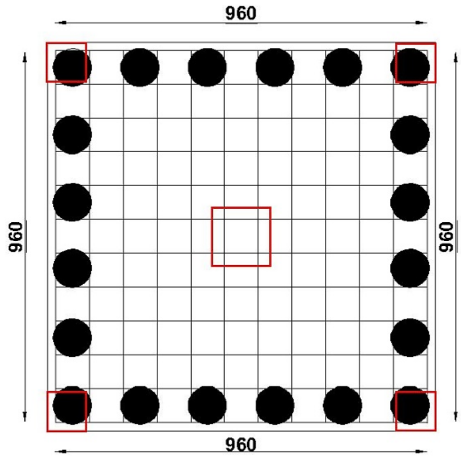

Fig. 3d: Arrangement of voids in 20VS8 and 20VS6.

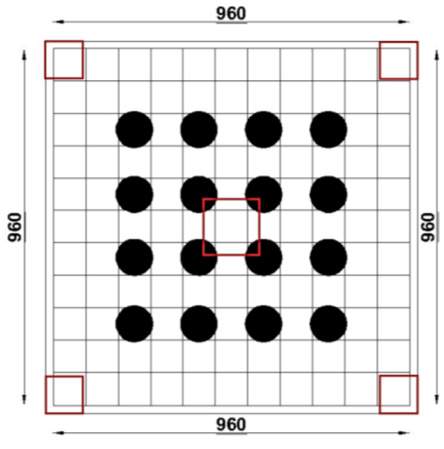

Fig. 3e: Arrangement of voids in 16VS8 and 16VS6.

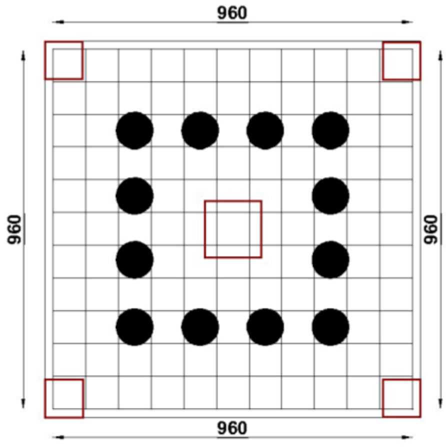

Fig. 3f: Arrangement of voids in 12VS8 and 12VS6.

3.2 Test setup and instrumentation

The vertical load test was conducted to study the structural behaviour of voided slabs. Figs. 4a and 4b show the schematic diagram and actual photograph of the actual test setup. The load was applied on the flat slab using a hydraulic jack in the loading frame of a capacity of 200 tons with a data acquisition system. The test specimens were supported with supports of size 100 mm × 100 mm × 50 mm on all four edges, as the voided slab is considered a flat slab without beams and with only columns. Linear variable differential transducer (LVDT) with a measuring range of ± 100 mm is provided at the centre of the slab to measure the mid-deflection at the mid-span of the slab, and the applied load was measured using a 500 kN capacity load cell. The arrangement of load cell and deflection gauges are shown in the schematic diagram of the Test Setup, Fig. 4. The real-time experimental data is obtained using a data acquisition system, with the facility to record load and deflections in the same instance.

3.3 Testing of specimens

A total of fourteen specimens (7 from each Group, i.e., Group-A and Group-B) were tested with 0, 36, 32, 24, 20, 16, and 12 number of voids up to failure. All specimens' dimensions were 1000 mm × 1000 mm ×150 mm with a short column size of 150 mm × 150 mm × 150 mm with regular reinforcement of 4 bars of 10 mm diameter with 8 mm diameter stirrups to avoid local crushing. All the slabs are reinforced with a double mat with a bar diameter of 6 mm in Group-A and 8 mm in Group-B. The high strength concrete cubes to avoid local failure with size of 100 mm × 100 mm × 50 mm were provided at all four corners below the test specimen to replicate the flat slab support conditions.

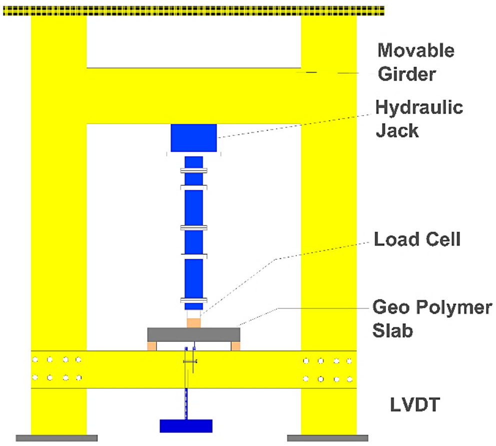

Fig. 4a: Schematic diagram of test setup.

Fig. 4b: Instrumentation of test specimen.

4 Results and discussion

The applied load *vs.* mid-deflection, stress *vs.* strain, and normalization curves were measured to assess the behaviour of the specimens under vertical load. A total of 14 flat slabs in two groups were cast and tested for failure; the same was validated with the finite element analysis method using ABAQUS software. Fig. 5, shows that the voided flat slab with zero voids 8 mm rebars (0VS8) have shown a higher load-carrying capacity of 220 kN with 3.31 mm mid-deflection. In comparison, 36VS8 has recorded relatively less load carrying capacity of 215 kN with 10.12 mm mid deflection, indicating that significant ductility index. Also, when the number of voids increases near the column, in specimens 36VS8, 36VS6, 24VS8, 24VS6, 16VS8, and 16VS6, it was observed the deflection magnitude gradually increases due to the ductile nature of specimens. It was evident that all specimens have shown yielding stress almost at the same load carrying capacity due to no impact of omitting the concrete in the tension zone of the flat slab below the neutral axis. Further, after the yield point, it was clearly shown in the response curves that the strain hardening zone indicates no pinching effect in the observed responses curve of 0VS8. From the Figs. 14–17, it is observed that the action of punching shear is relatively less in the specimens with the voids placed away from the column and supports. 12VS8, and 12VS6, are the specimens with voids placed away from the column and supports. 0VS8 and 0VS6 has zero voids. All the flat slabs failed almost the same magnitude of load in that particular Group-A and Group-B. Rest of the flat slabs have shown relatively more deflection at the same load because of the punching load.

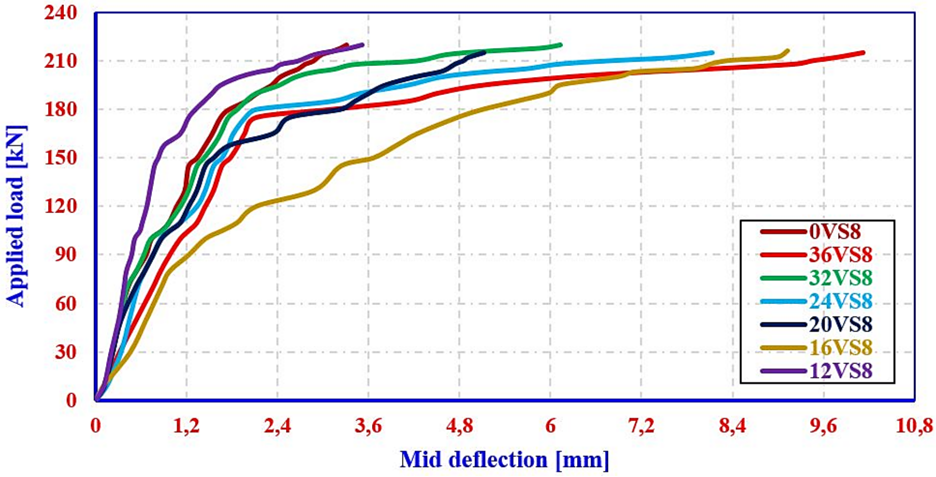

Fig. 5: Applied load *vs.* mid deflection of all specimens, Group-B.

The current parametric study shows up to 36 voids can be formed in the tested slabs as an optimized void ratio. The crack pattern of all specimens was punching shear at the centre as shown in Fig. 6. The yield line cracks have been noticed as shown in Figs. 18-21. Similar type of punching shear effect has been observed in all tested specimens.

Fig. 6: Punching shear at the centre of the tested voided flat slab.

Fig. 7 shows that the flat slab with zero voids had shown a higher load-carrying capacity of 152 kN with 3 mm mid-deflection. In comparison, 36VS6 has recorded relatively less load carrying capacity of 145 kN with 9 mm indicating that significant ductility index. Similar to 8 mm reinforcement slabs, it was noticed that when the number of voids increases, the deflection gradually increased due to the ductile behaviour of the specimens. It was noticed that all specimens yielding behaviour were almost at the same load-carrying capacity due to no impact of omitting the concrete in the tension zone of the flat slab below the neutral axis. Further, after the yield point, it was clearly shown in the response curves that the strain hardening indicated no pinching effect in the tested specimens.

As per as current parametric study concern, up to 36 voids can be formed in the tested slabs as an optimized void ratio similar to 8 mm rebar specimens. The crack pattern of all specimens was punching shear at the centre, Fig. 6. At supports yield line cracks were noticed, Figs. 18-21. The pre-peak and post-peak behaviour of all slabs, both 8 mm and 6 mm rebars, have shown relatively significant results, indicating that ample warning before failure of the test specimens.

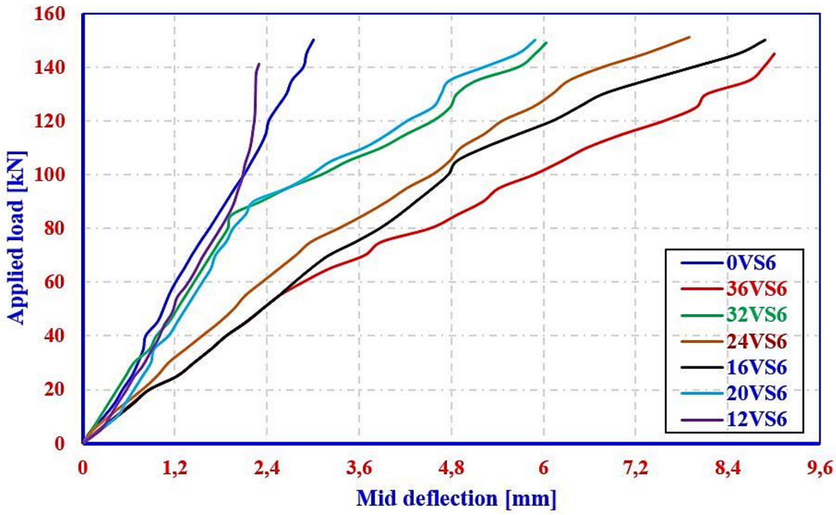

Fig. 7: Applied load *vs*. mid deflection of all specimens, Group-A.

4.1 Stress vs. strain behaviour

The stress was found with the ratio of applied load (obtained from experimental test results) to the area of the cross-section of the slab i.e., 1000 mm × 150 mm (obtained from actual dimensions of test specimen) and the strain was found with ratio of each mid-deflection of the specific slab to the thickness of the slab i.e., 150 mm. It is direct process of calculating stress-strain behaviour from applied load *vs.* mid deflection curves.

From Fig. 8, it was observed that the slab with zero voids failed after the elastic limit with corresponding strain occurring at 1.75 %. 0VS8, the response curve varied linearly up to the stress of 9.86 MPa, with the corresponding strain at 3.35 % and leading to failure. Slab 36VS8, it was observed that strain was constant till it reached the stress of 8.44 MPa, and later curvature was linear up to the stress of 9.68 MPa with the corresponding strain at 3.35 %. In slab 32VS8, it was observed that strain was constant till it reached stress of 9.33 MPa and later varied linearly up to stress at 9.42 MPa and corresponding strain at 4.16 % and leading to strain hardening.

In slab 24VS8, it was noticed that strain was constant till it reached the stress of 8.22 MPa with the corresponding strain at 3.21 %. In slab 20VS8, it was noticed that strain was constant till it reached to the stress of 8 MPa with the corresponding strain at 3.23 %. In slab 16VS8, it was noticed that strain was constant till it reached the stress of 9.21 MPa with the corresponding strain at 8.12 %. In slab 12VS8, it was noticed that strain was constant till it reached the stress of 9.51 MPa with the corresponding strain at 2.89 %.

From Fig. 9, it was observed that the slab with zero voids failed after the elastic limit with corresponding strain occurring at 2.72 %. 0VS6, the curve varied linearly up to the stress of 6.00 MPa, with the corresponding strain at 2.82 % and leading to failure. Slab 36VS6, it was observed that strain was constant till it reached the stress of 3.33 MPa, and later curvature was linear up to the stress of 3.45 MPa with the corresponding strain at 3.89 %.

In slab 32VS6, it was observed that strain was constant till it reached a stress of 3.70 MPa and later varied linearly up to stress at 3.86 MPa and corresponding strain at 1.89% and leading to strain hardening. In slab 24VS8, it was noticed that strain was constant till it reached the stress of 3.33 MPa with the corresponding strain at 2.98 %.

In slab 20VS8, it was noticed that strain was constant till it reached the stress of 4.00 MPa with the corresponding strain at 2.23 %. In slab 16VS8, it was noticed that strain was constant till it reached the stress of 3.11 MPa with the corresponding strain at 3.21 %. In slab 12VS8, it was noticed that strain was constant till it reached the stress of 6.00 MPa with the corresponding strain at 2.56 %.

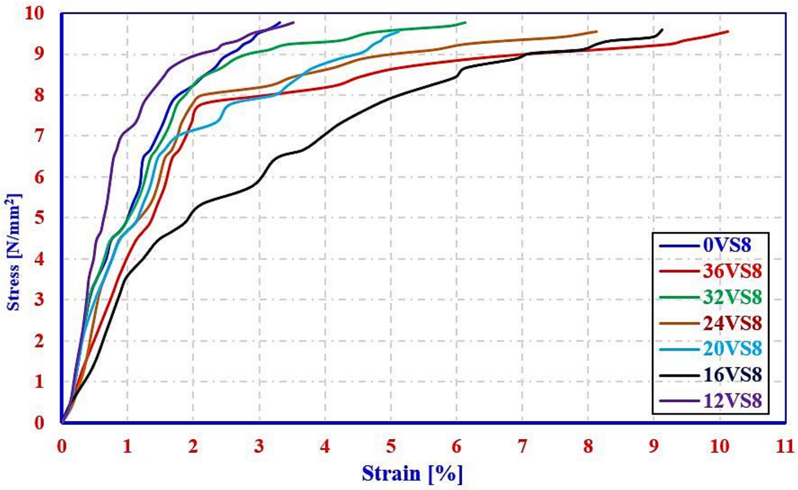

Fig. 8: Stress *vs.* strain responses of all specimens, Group-B.

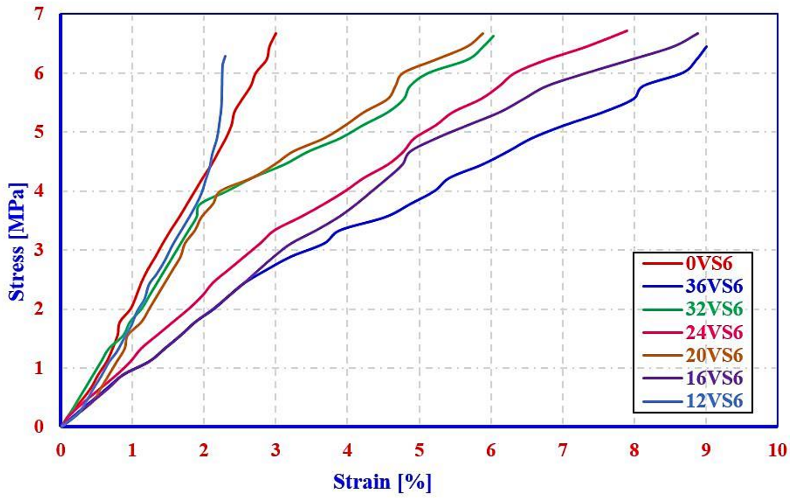

Fig. 9: Stress *vs.* strain responses of all specimens, Group-A.

4.2 Normalization behaviour

From the Fig. 10, each vertical load on the specific slab is normalized, by the product of the compressive strength of concrete and area of concrete f_{ck}×*b*×*t* (i.e., *b* - breadth of slab and *t* - thickness of slab), whereas each mid deflection was normalized with a thickness of the slab $^{\Delta}/_{t}$, where Δ is mid deflection of test specimens and *t* is the thickness of the slab against the normalized vertical load. This normalization process has done for further parametric study by any researcher on voided flat slabs. It can be observed that the contribution of the shear force ratio was relatively higher for the slab with zero voids. However, the shear force ratio was relatively low for slab 36VS8.

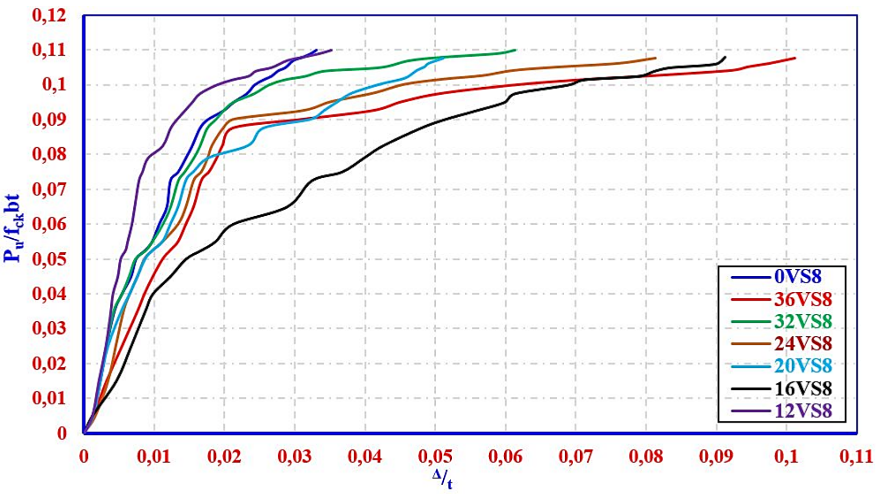

Fig. 10: Normalization curves of all Specimens, Group-B.

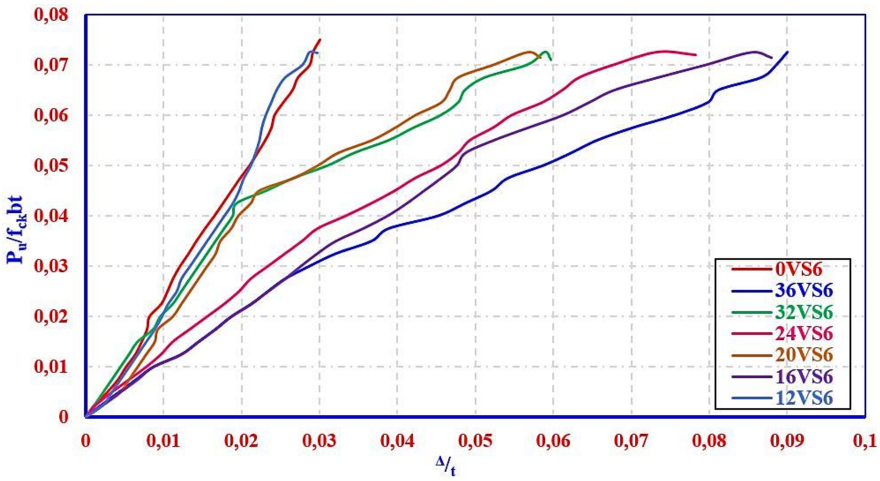

Fig. 11: Normalization curves of all specimens, Group-A.

Similar to 8 mm, from Fig. 11, each vertical load on the specific slab is normalized, by the product of the compressive strength of concrete and area of concrete $f_{ck} \times b \times t$, where each mid deflection is normalized with a depth of the beam $^{\Delta}/_{t}$, against the normalized vertical load. It can be observed that the contribution of the shear force ratio was relatively higher for the slab with no voids. However, the shear force ratio was found to be low for slab 16VS6.

5 Numerical study

Analytical models are also developed in addition to the experimental investigations for a more in depth understating of voided flat slabs and validation of experimental results. To evaluate the nonlinear geometric and material behaviour of both concrete and steel, a 3D finite element model was created in ABAQUS.

ABAQUS concrete damaged plasticity model [17] provides the general capability of modelling concrete and quasi-brittle materials in all types of structures like beams, trusses, shells, and solids to represent the inelastic behaviour of concrete [18]. An isotropic damage elasticity in combination with isotropic tensile and compressive plasticity concepts were used. The model is a continuum, plasticity-based model for concrete. The ABAQUS model assumes that concrete uniaxial tensile and compressive responses are characterized by damaged plasticity. The response of concrete to uniaxial loading in tension and compression (σ_t and σ_c are tensile and compressive stresses & ε_t, ε_c are tensile and compressive strains), where d_t and d_c are two scalar damage variables, ranging from 0 (undamaged) to 1 (fully damaged) where the subscript '*c*' refers to compression and *t* represents tension. The damaged model used for concrete was based on plasticity and considered the failure process of tensile cracking and compressive crushing have shown in Figs. 12 and 13 [19]. The primary aim of the numerical modelling was to determine the overall load carrying capacity of the flat slab and to analyse its failure. Due to the specification of the analysis, 3D computational models were used [20].

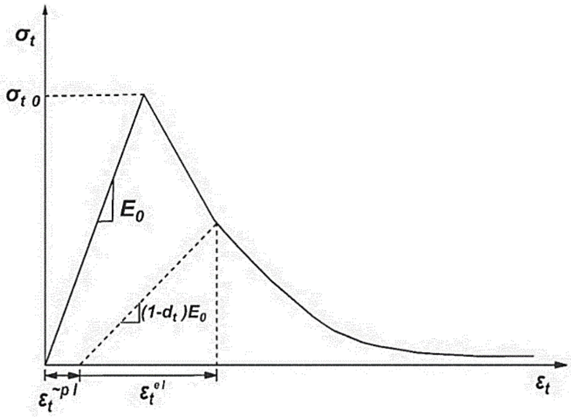

Fig. 12: Response of concrete to uniaxial loading in tension.

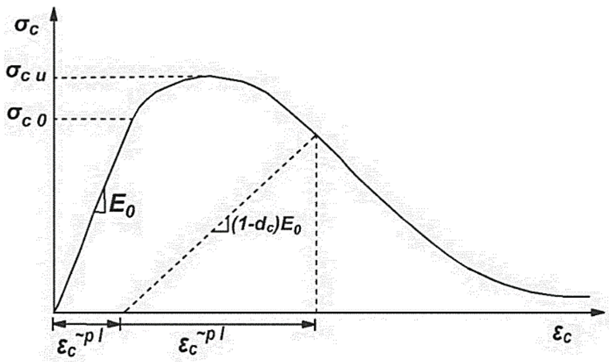

Fig. 13: Response of concrete to uniaxial loading in compression.

The stress-strain response follows a linear elastic relationship until the value of failure stress, σ_{t0}, is reached. With softening stress-strain response, the micro-cracks are represented beyond the failure stress, which induces strain localization in the concrete structure. Until the value of the initial yield σ_{c0} beyond the ultimate stress, σ_{cu} in the plastic regime, the response is typically characterized by stress hardening followed by strain softening. If E_0 is the initial (undamaged) elastic stiffness of the material, the stress-strain relation under uniaxial tension represents as eq. (1).

$$\sigma_t = (1-d_t)E_o(\varepsilon_t - \varepsilon_t^{\sim Pl}), \quad (1)$$

and the stress-stain relation under uniaxial compression given in eq. (2)

$$\sigma_c = (1-d_c)E_o(\varepsilon_t - \varepsilon_t^{\sim Pl}), \quad (2)$$

where the subscript *c* refers to compression and *t* represents tension and $\varepsilon_t^{\sim Pl}$, $\varepsilon_c^{\sim Pl}$ are equivalent plastic strains while effective tensile and compressive cohesion stresses are shown in eqs. (3) and (4)

$$t = \frac{\sigma_c}{(1-d_c)} = E_o\left(\varepsilon_t . \varepsilon_t^{\sim Pl}\right), \quad (3)$$

$$t = \frac{\sigma_c}{(1-d_c)} = E_o\left(\varepsilon_c . \varepsilon_c^{\sim Pl}\right), \quad (4)$$

The values of the cracking strain were automatically converted via programming to plastic strain values according to eqs. (5) and (6) with the availability of unloading data.

$$\varepsilon_t^{\,Pl} = \varepsilon_t^{\,ck} \frac{d_t}{(1-d_t)} \frac{f_t}{E_t}, \quad (5)$$

$$\varepsilon_c^{\,Pl} = \varepsilon_c^{\,ck} \frac{d_c}{(1-d_c)}. \quad (6)$$

The modulus of concrete elasticity was calculated as per formulae $E_c = 500\sqrt{f_{ck}}$ MPa where f_{ck} is the compressive strength at 28 days.

To simulate, the behaviour of slab three-dimensional modelling was adopted. Eight-noded hexahedral element C3D8R was used to represent the concrete and steel bar modelled by using the truss element T3D2 with two nodes. The embedded option assumed a perfect bond between the concrete and reinforcement. The supports were shaped using a rigid discrete part, and bilinear quadrilateral elements R3D4 with four nodes were employed in meshing them. To arrest the translations and movements in all directions, support conditions were assigned. Indeed, this option was accurate compared to real tests of RC elements, and it avoids the numerical non-convergence issue due to adopting complicated interaction options [21].

CDPM parameters as stated formerly, the CDPM contains five factors to define the plasticity of concrete. Three (viscosity, dilation angle and shape factor) must be adjusted to get the best FEA simulations. The viscosity parameter μ is used to overcome the convergence issue that encounters the materials simulation of softening behaviour and stiffness degradation. This issue arises when using ABAQUS/Standard, whereas it becomes unimportant with employing ABAQUS/Explicit.

The correlation between the load-deflection curve of the Finite Element (FE) analysis and that of the test is considered the critical aspect in achieving the validation of FE model since this curve includes the response parameters like yield and ultimate loads, maximum deflection, ductility, stiffness, and energy absorption [22].

To reach this goal, two out of five CDPM parameters (dilation angle and viscosity) as well as the mesh size, were investigated carefully. After a sensitive analysis, the mesh size of 5 mm was adopted, while the dilation angle and viscosity were selected to be 20° and 0.005, respectively. For the remaining three parameters of CDPM, which are eccentricity, shape factor, and stress ratio, the default values were chosen, which are 0.1, 1.16, and 0.667, respectively, as followed by previous numerical investigations conducted on the punching shear in flat slab [23].

6 Validation

Validation of experimental results with the numerical results for a better understanding of voided flat slabs structural behaviour. The value of the observed deflections is compared with the corresponding finite element models of the same tested voided flat slab. Figs. 14 and 15 illustrates the comparison of applied load *vs.* mid-deflection responses of experimental and numerical (Group-B), whereas Figs. 16 and 17, present the comparison of applied load *vs*. mid-deflection responses of experimental and numerical results (Group-A). The deflection values are inversely proportional to the rate of steel. With the increasing wire mesh diameter from 6 mm to 8 mm, the deflections decreased compared with Group- A and Group-B. Group-B voided slabs ultimate load-carrying capacity is higher when compared to Group-A. The load-carrying capacity of Group-A and Group-B voided flat slabs is nearly the same in that particular Group. The slab deflections vary depending on the distance of placing voids from the face of the short column (which was constructed for the application of load) and supports. The punching shear is acting till a distance of 0.5d from the face of the column and the support.

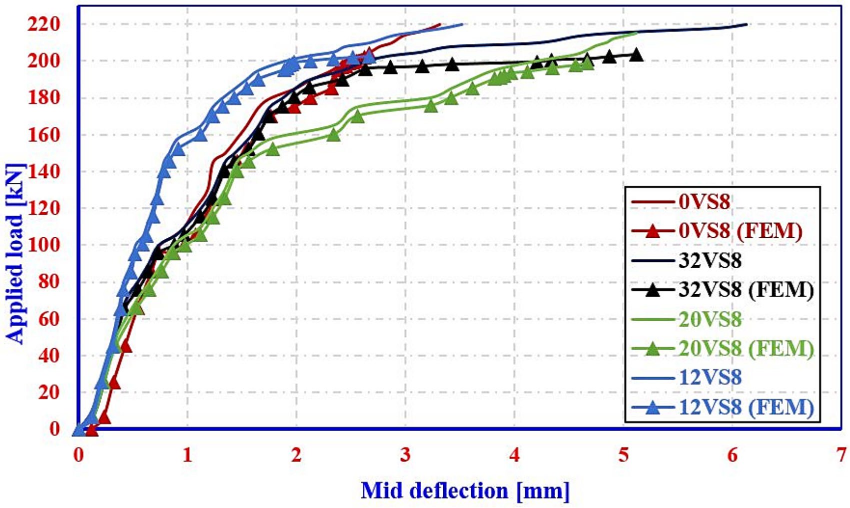

Fig. 14: Comparison of applied load *vs.* mid deflection responses of experimental and numerical Group-B (0VS8, 32VS8, 20VS8 and 12VS8).

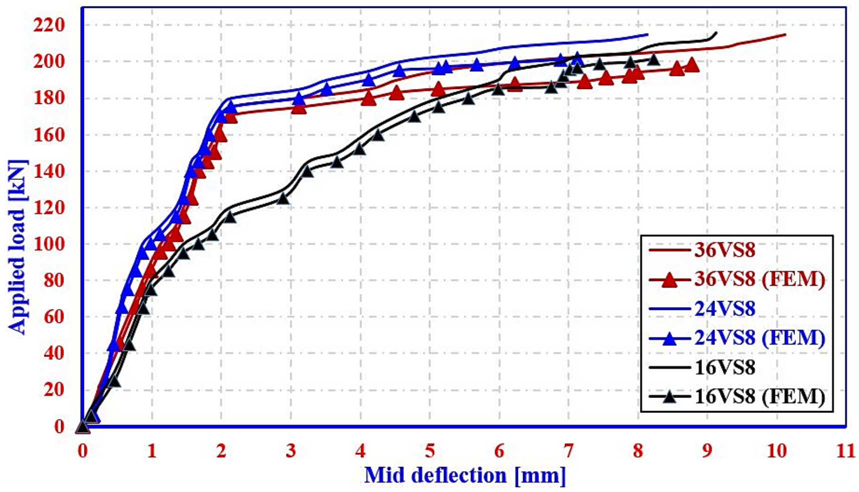

Fig. 15: Comparison of applied load *vs*. mid deflection responses of experimental and numerical Group-B (36VS8, 24VS8 and 16VS8).

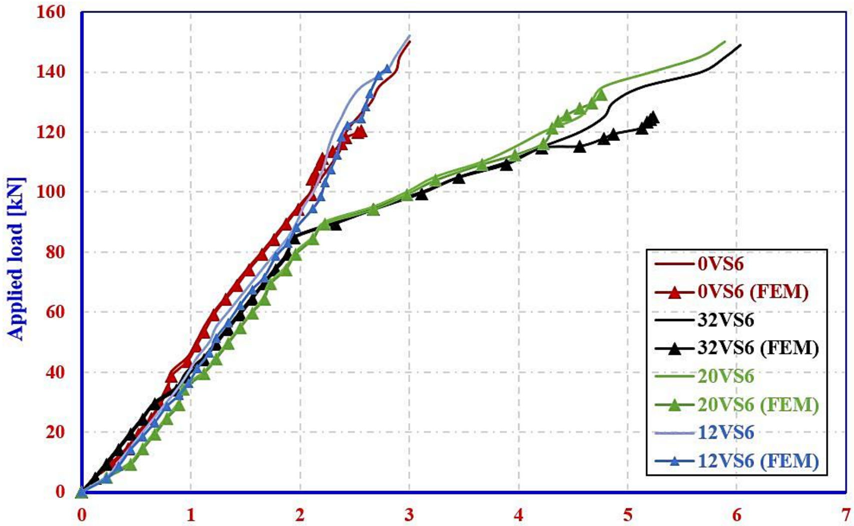

Fig. 16: Comparison of applied load *vs.* mid deflection responses of experimental and numerical Group-A (0VS6, 32VS6, 20VS6 and 12VS6).

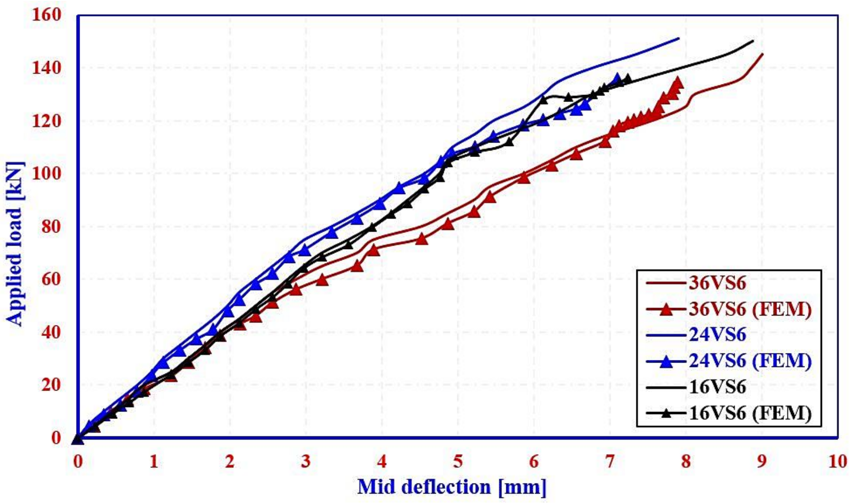

Fig. 17: Comparison of applied load *vs.* mid deflection responses of experimental and numerical

6.1 Failure load and crack pattern

The initial and final crack patterns of voided flat slabs have shown in Figs. 18 and Fig. 19. The crack pattern for all configurations of slabs has shown similar nature. Fig. 20 shows the yield line crack pattern of a voided flat slab 8 mm, whereas Fig. 21 shows the yield line crack pattern of a voided flat slab 6 mm. Fig. 22 shows the deflection contour of 36VS8. Fig. 23 shows the stress contour of 36VS8. Fig. 24 shows tensile damage of 36VS8, whereas Fig. 25: visualization of specimen 36VS8.

Fig. 18: Yield line crack pattern of voided flat slab (Initial crack).

Fig. 19: Yield line crack pattern of voided flat slab (Final crack).

Fig. 20: Yield line crack pattern of voided flat slab (36VS8).

Fig. 21: Yield line crack pattern of voided flat slab (36VS6).

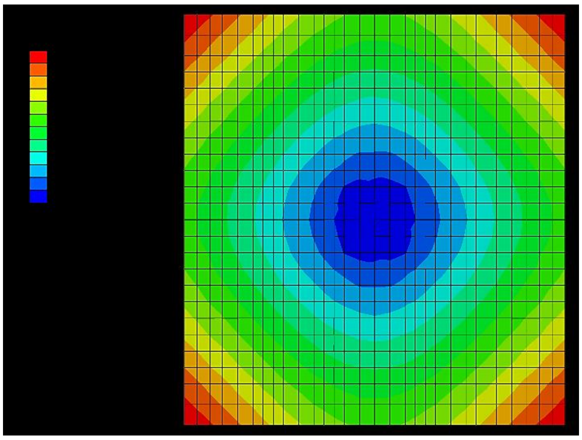

Fig. 22: Deflection contour of 36VS8.

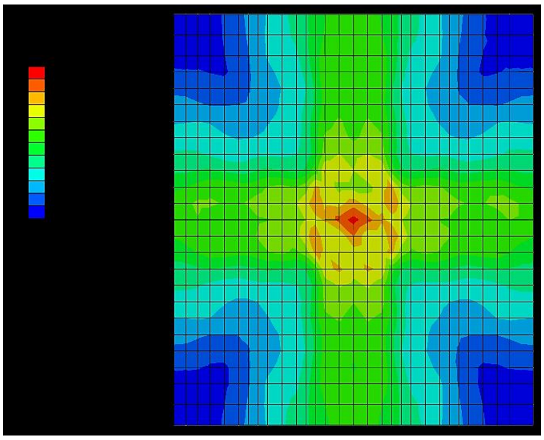

Fig. 23: Stress contour of 36VS8.

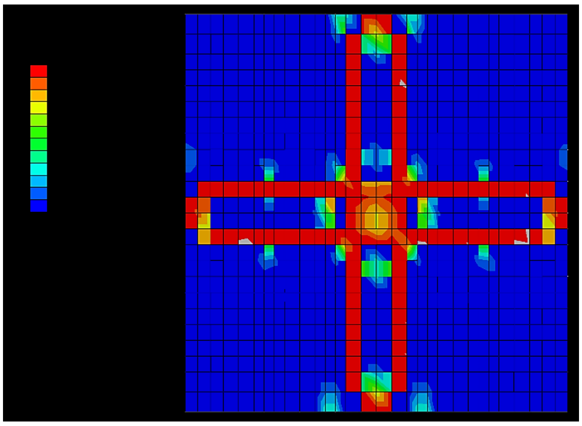

Fig. 24: Tensile damage of 36VS8.

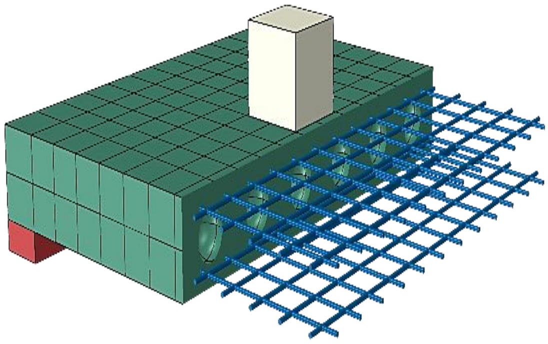

Fig. 25: Visualization of specimen 36VS8.

7 Conclusions

The present study investigates the structural behaviour of voided flat slabs under vertical loading. To have an awareness of voided slabs, a method of virtually eliminating the structurally not functioning concrete using recycled HDPE voids, thereby reducing self-weight and increasing the efficiency of the floor. The following conclusions have been drawn from the observations of experimental and numerical studies.

1) Voided flat slabs have the tremendous advantage of reducing the dead load (self-weight of slab) on columns, walls and foundations, due to this the structure become more sustainable.
2) The voided slabs with 6 mm and 8 mm reinforcement showed promising results, which are very near to the conventional slab.
3) The percentage of voids did not affect the load-carrying capacity of the voided slab as replaced the non-functioning concrete using the HDPE voids.
4) On the other hand, the position of the voids plays a crucial role in punching shear of the slab.
5) The crack pattern on all category of slabs have shown the replication of yield line cracks.
6) The punching is occurred exactly at the centre on top of the slab where the load is being applied, similarly at the bottom proximity of the supports.
7) The crack pattern being noticed differently in all flat slabs when compared to simply supported slab (where most of the research has been encountered) from previous research.
8) The experimental and numerical results found almost same with minimum deviation.
9) In this current study, the HDPE hollow sphere manufactured from recycled plastic, which are used to replace the concrete below the neutral axis is environmentally friendly.

The following future scope shall be undertaken as future challenges of this current research:

1) Experimental studies on structural behaviour of voided flat slabs by providing extra reinforcement at the supports.
2) Experimental studies on strengthening voided flat slabs using CFRP and GFRP.
3) Sustainable studies on the voided flat slabs using fly ash based Geopolymer concrete.

Acknowledgment

Dr. P. Poluraju is to be thanked for his valued supervision throughout the experimental work, for inspiring the author to keep going even when things became tough, for ongoing project monitoring, and for helping with the development of the study proposal.

References

[1] CHURAKOV, A.: Biaxial hollow slab with innovative types of voids. Construction of Unique Buildings and Structures, Vol. 6, 2014, pp. 70-88.
[2] Teja, P. P. - Vijay, K. P. - Anusha, S. - Mounika, C. H. - SAHA, P.: Structural Behaviour of Bubble Deck Slab. IEEE-International Conference on Advances in Engineering, Science and Management, ICAESM -2012, 2012, pp. 383-388.
[3] SAGADEVAN, R. - RAO, B. N.: Experimental and Analytical Investigations on Two-way Flexural Capacity of Biaxial Voided Slab. Proceedings of National Conference on Advances in Structural Technologies, CoAST-2019, 2019, pp. 635-648.
[4] HUSSEIN, L. F. - Al-TAAI, A. A. S. - KHUDHUR, I. D.: Sustainability achieved by using voided slab. 2nd International Conference on Materials Engineering & Science, IConMEAS 2019, 2019, pp. 020071-1-020071-7, https://doi.org/10.1063/5.0000216.
[5] LAI, T.: Structural Behaviour of Bubble Deck Slabs and Their Application to Lightweight Bridge Decks, 2010.
[6] RAGEH, M. O. - HOSNY, H. – REHEM, A. A.: Sustainability Requirements of Concrete Structures, American Journal of Civil Engineering and Architecture, Vol. 5, 2017, No. 5, pp. 174-186, doi:10.12691/ajcea-5-5-1.
[7] CHUNG, J. H. - CHOI, H. K. - CHOI, C. S. – JUNG, H. S.: Punching Shear Design Method of Voided Slabs. Key Engineering Materials, Vol. 754, 2017, pp. 754-333, https://doi.org/10.4028/www.scientific.net/KEM.
[8] CHUNG, J. H. - CHOI, H. K. - LEE, S. C. - CHOI, C. S.: Shear capacity of biaxial hollow slab with donut type hollow sphere. Procedia Engineering, Vol. 14, 2011, pp. 2219-2222, https://doi.org/10.1016/j.proeng.2011.07.279.
[9] FALAH, H. - ADNAN, D.: Punching Shear Behavior of fibrous high strength concrete slabs reinforced with BFRP bars. Civil and Environmental Engineering, Vol. 18, No. 2, 2022, pp. 565-580, doi: 10.2478/cee-2022-0054.
[10] SAGADEVAN, R. - RAO, B. N.: Experimental and Analytical Investigations on Two-way Flexural Capacity of Biaxial Voided Slab. National Conference on Advances in Structural Technologies, CoAST-2019, 2019, pp. 635-648.
[11] HAI, L. V. - HUNG, V. D - THI, T. M. - THOI, T. N. - PHUOC, N. T. : The Experimental Analysis of Bubble Deck Slab Using Modified Elliptical Balls Proceedings of the Thirteenth East Asia-Pacific Conference on Structural Engineering and Construction, EASEC-13, 2013, Sapporo, Japan, G-6-1., G-6-1, pp. 1-9.
[12] AL-GASHAM, T. S. - MHALHAL, J. M. - ABID, S. R.: Quasi-static analysis of biaxial voided slabs with openings. Structures, 2021, Vol. 33, pp. 4176–4192, https://doi.org/10.1016/j.istruc.2021.07.021.
[13] SAGADEVAN, R. - RAO, B. N.: Numerical Study on Punching Shear Capacity of Biaxial Hollow Slabs. 5th International Congress on Computational Mechanics and Simulation, ICCMS-2014, 2014, pp. 1881-1890.
[14] IS 10262-2019. Concrete Mix Proportioning — Guidelines, Bureau of Indian Standards, New Delhi.
[15] IS 456:2000. Plain and Reinforced Concrete-Code of Practice. Bureau of Indian Standards, New Delhi.
[16] IS 1608 Part 1: 2018, Metallic Materials - Tensile Testing at Ambient Temperature. Bureau of Indian Standards, New Delhi.
[17] Hafezolghorani, M. - Hejazi, F. - Vaghei, R. - Jaafar, M. S. B. - Karimzade, K.: Simplified Damage Plasticity Model for Concrete. Structural engineering international, 2017, pp. 68-78, doiI:10.2749/101686616X1081.
[18] KOZIELOVA, M. – MARCALIKOVA, Z. – MATECKOVA, P. – SUCHARDA, O.: Numerical analysis of Reinforced Concrete slab with subsoil. Civil and Environmental Engineering, Vol. 16, Iss. 1, 2020, pp. 107-118, doi: 10.2478/cee-2020-0011.
[19] SMITH, M.: ABAQUS/Standard User's Manual, Version 6.9, Dassault Systèmes Simulia Corp, 2009.

[20] MARCALÍKOVA, Z. - CAJKA, R: Numerical Modelling and Diagnostic of FRC Slab under centric and eccentric load. Civil and Environmental Engineering, Vol. 18, Iss. 1, 2022, pp. 17-28, doi: https://doi.org/10.2478/cee-2022-0002.
[21] NAVARROA, M. – IVORRAA, S. – VARONA, F. B.: Parametric computational analysis for punching shear in RC slabs. Engineering Structures, Vol. 165, 2018, pp. 254-263, https://doi.org/10.1016/j.engstruct.2018.03.035.
[22] MARCALÍKOVA, Z. - CAJKA, R: Determination of Mechanical Properties of Fibre Reinforced Concrete for Numerical Modelling. Civil and Environmental Engineering, Vol. 16, Iss. 1, 2020, pp. 86-106, doi: https://doi.org/10.2478/cee-2020-0010.
[23] Genikomsou, A. S. - Polak, M. A.: Finite Element Analysis of Punching Shear of Concrete Slabs using Damaged Plasticity Model in ABAQUS. Engineering Structures, Vol. 98, 2015, pp. 38-48, http://dx.doi.org/10.1016/j.engstruct.2015.04.016.